Global Ecology and Biogeography

WILEY

Global Ecology and Biogeography
A Journal of Macroecology

METHOD OPEN ACCESS

Simulating and Analysing Seabird Flyways: An Approach Combining Least-Cost Path Modelling and Machine Learning

Nomikos Skyllas[1,2,3] | Mo A. Verhoeven[4,5] | Maarten J. J. E. Loonen[6] | Richard Bintanja[1,2]

[1]Energy and Sustainability Research Institute Groningen (ESRIG), University of Groningen, Groningen, the Netherlands | [2]Royal Netherlands Meteorological Institute (KNMI), De Bilt, the Netherlands | [3]Institute for Biodiversity and Ecosystem Dynamics (IBED), University of Amsterdam, Amsterdam, the Netherlands | [4]Department of Coastal Systems, NIOZ Royal Netherlands Institute for Sea Research, Utrecht University, Texel, the Netherlands | [5]Department of Animal Ecology, Netherlands Institute of Ecology (NIOO-KNAW), Wageningen, the Netherlands | [6]Arctic Centre, University of Groningen, Groningen, the Netherlands

Correspondence: Nomikos Skyllas (n.skyllas@rug.nl)

Received: 14 May 2024 | **Revised:** 10 February 2025 | **Accepted:** 16 February 2025

Handling Editor: Manuel Steinbauer

Funding: This publication is part of the project *Vulnerability of Arctic migratory birds to rapid climate change* with project number ALWPP.2019.007 of the research programme NPP, which is (partly) financed by the Dutch Research Council (NWO).

Keywords: climate | cost | effort | flight | flyway | least cost path | minimisation

ABSTRACT

Aim: We develop and test a cost framework to simulate the flyways of migratory seabirds, considering various environmental factors such as wind support, crosswind, travel distance, and food availability. Using this framework, we simulate potential migratory flyways for arctic terns and compare these simulations with tracking data. Our aim is to identify which combination of factors best explains the observed flyways. Ultimately, we seek to demonstrate how different environmental factors shape flyways.

Innovation: We simulated 195 possible seabird flyways using a newly developed cost function that takes into account a number of environmental variables. We focused on the Arctic Tern, a transhemispheric migrating seabird species. Our model accurately simulated most spring and autumn flyways across the Atlantic Ocean (median RMSE ± standard deviation for all five flyways: 529 ± 201 km). The most accurate simulations for Arctic Terns breeding on Svalbard were those for which wind support made up ~70% of the total cost, while the best simulations for the Dutch population were those for which distance minimisation was ~50% and food maximisation was ~30% of total costs. Finally, by analysing tracking data using a machine-learning algorithm factoring in both wind support and crosswind, we were able to determine airspeed and subsequently infer whether the observed flyways optimised time and/or effort.

Main Conclusions: This analysis showed that Arctic Terns breeding on Svalbard followed effort-optimising flyways, whereas those that breed in the Netherlands followed time-optimising flyways. Our simulation-to-observation approach demonstrates that Earth's environmental and physical properties likely underlie the global distribution of migratory birds and therefore need to be considered in studies that evaluate the long-range movement patterns and distribution of birds.

1 | Introduction

A flyway is the full geographic range that a migratory bird species (or groups of related species or different populations within the same species) travels each year, moving from breeding areas to non-breeding habitats (Boere et al. 2006). At the global scale, the location of flyways is related to the configuration of oceans and continents, and to natural barriers (e.g., deserts, mountain ranges) and corridors (e.g., rivers, valleys) of the landscape. At a finer spatial scale, the main environmental drivers shaping a given flyway are wind conditions and food availability (Safi et al. 2013; Lisovski et al. 2021). Migratory birds require sufficient resources before, during, and after their migration in order to successfully complete the migration, maintain their reproductive output, and avoid population decline (Weber et al. 1998; Prop et al. 2003; Rakhimberdiev et al. 2018). Energy expenditure during flight is decreased by tailwinds and increased by headwinds and crosswinds (Kranstauber et al. 2015; Loonstra et al. 2019). As a result, flyways are usually paths that offer short routes and/or favourable wind conditions while also providing the resources necessary to complete a migration.

Previous studies have successfully used a framework of cost minimisation to understand why certain flyways are used. For instance, Felicísimo et al. (2008) and González-Solís et al. (2009) simulated the migration of three shearwater species (*Manx Puffinus puffinus, Calonectris diomedea*, and *Calonectris edwardsii*) over the Atlantic Ocean by using cost functions that rewarded movements supported by tailwinds. Similarly, Kranstauber et al. (2015), Loonstra et al. (2019) and Lisovski et al. (2021) used prevailing wind conditions to simulate bird migration with a function that minimised time and consequently maximised survival. They either connected the flight time to the wind-induced flight cost and consequently to an increased risk of in-flight mortality (Loonstra et al. 2019) or assumed that travel time has a sigmoidal relationship with mortality (Kranstauber et al. 2015; Lisovski et al. 2021). These studies support the idea that flyways reflect the circumstances in which birds can perform successful migrations.

While it is possible to use such least-cost-path modelling approaches to simulate bird flyways (e.g., Kranstauber et al. 2015; Lisovski et al. 2021), a major challenge is deciding which costs these models should minimise. To date, most studies have focused on the effects of wind, particularly tailwind. In accordance with optimal migration theory (Alerstam and Lindström 1990)—which suggests that birds aim to minimise the total cost of migration by balancing energy expenditure, time, and risk—these models have primarily focused on minimising either time or effort. Tailwinds can reduce energy expenditure, shorten travel duration, and ultimately influence survival and reproduction by allowing an animal to conserve energy. Although these studies have yielded valuable insights into why certain wind-supported flyways are used (Vansteelant et al. 2017; Norevik et al. 2019), they have also revealed that some birds use flyways that seem less optimal in terms of wind support (Loonstra et al. 2019; Lisovski et al. 2021).

The fact that migratory birds follow flyways other than the most wind-supported ones suggests that a broader range of factors and strategies is at play, beyond merely optimising wind support. A notable contribution to this understanding is the study by Revell and Somveille (2017), who developed a mechanistic model simulating bird movements away from a location and across a potential landscape shaped by two environmental variables: chlorophyll a and wind support. Their approach, akin to least-cost-path modelling, was successfully used to simulate the movements of black-browed albatrosses (*Thalassarche melanophris*). An interesting next step would be to include even more environmental factors in addition to wind support and food availability (e.g., Lisovski et al. 2021). Expanding our understanding by including factors such as crosswinds and travel distance will also improve our ability to accurately assess the influence of global change on flyways. However, including more environmental factors will also present new challenges related to disentangling complexity: (1) to what extent does each factor determine if a flyway is used by migratory birds; (2) what outcome is optimised as a result of combining different factors in different ways; and (3) how do these outcomes relate to the traditional frameworks of time, energy and risk minimisation?

Here we develop and test a multi-factor cost framework to simulate least-cost paths for many different combinations of wind support, crosswind, travel distance and food optimisation. We use this framework to simulate potential migratory flyways for a seabird species that migrates across the Atlantic Ocean: the Arctic Tern (*Sterna paradisaea*). We use geolocator data to track these birds and determine which simulated flyway, and thus which combination of the four environmental factors, best matches the observed flyways. Hence, we employ a simulation-to-observation approach which differs from the more usual observation-to-simulation approach of tracking individual birds and then trying to understand the resulting tracks. From the geolocator tracking, we also infer the birds' response (airspeed regulation) to wind conditions by using a machine-learning algorithm. Finally, by annotating the simulated flyways with wind data and applying the inferred bird's response, we show that different flyways form as the result of different responses to the environment, and in consequence different costs are minimised.

2 | Methods

2.1 | The rWind Package

rWind is an R language package that allows the user to compute wind connectivity between locations (for a detailed description, see Fernández-López and Schliep 2019). It uses friction layers: maps of a geographical/ecological characteristic that may influence dispersal or movement ability. It then applies the Dijkstra algorithm (Dijkstra 1959) to compute the Least Cost Path (LCP) between two points. When using gridded wind data, the cost between two positions depends on the wind speed and wind direction of the source grid cell and on the location of the target grid cell. To compute this cost, the rWind package implements by default the algorithm proposed by Muñoz et al. (2004) and the update by Felicísimo et al. (2008).

$$\text{cost} = \frac{\text{HF}}{S} \qquad (1)$$

$$\text{HF} = \begin{cases} 0.1, & \text{HRMA} = 0 \\ 2 \times \text{HRMA}, & \text{HRMA} \neq 0 \end{cases}$$

Where S is the wind speed and HRMA is the horizontal relative moving angle (the angle in degrees between the wind direction and the direction of the movement trajectory to the target cell). Finally, HF is the horizontal factor (a function of the HRMA).

We find that this cost formula results in questionable costs in some cases. For example, flying into strong headwinds leads to lower costs than following weak tailwinds (Figure S1). Dividing the HF by wind speed results in reasonable cost values only for tailwinds: weak tailwinds have higher costs than strong tailwinds. However, in the case of crosswinds and headwinds, strong winds illogically result in lower costs than weak winds, and as a result the simulated birds will primarily follow strong cross- and headwinds (in addition to tailwinds). In this study we will develop a new (multi-component) cost formula (see details below), which we use in combination with the rWind package, avoiding the above-mentioned issues with the original cost formula, and leading to more realistic results for a wide range of bird flight behaviours. Our cost formula relies on two types of environmental data: wind and chlorophyll a (a proxy for food).

2.2 | The Cost Formula

2.2.1 | 1st Component: Standardised Parallel Wind Cost

The first component of the cost formula is the "standardised parallel wind cost" (w_cost), which calculates the wind-induced cost of movement from the source cell (I) to the target cell (j), on a 2-dimensional surface, using the following formula:

$$\text{windsupport}_{\text{i,j}} = |\vec{w}|_i \times cos\theta_{i,j}$$

$$\text{parallel wind cost}_{i,j} = |\text{windsupport}_{\text{i,j}} - P_{99}(\text{windsupport})|$$

$$\text{standardised parallel wind cost}_{i,j} = \frac{100}{P_{99}(\text{parallel wind cost})} \times \text{parallel wind cost}_{i,j} \tag{2}$$

where $|\vec{w}|$: wind speed (magnitude of wind vector), i: the source cell, j: the target cell and θ: the angle between the wind vector ($\vec{w}$) and the bird's groundspeed ($\vec{g}$).

This component focuses on the axis parallel to the bird's movement and calculates the wind support that a bird experiences when moving between two cells ($|\vec{w}| \times \cos\theta$), resulting in movements with tailwinds (high positive values of wind support in m/s), headwinds (high negative values) and very weak winds or crosswinds (close to zero). It then subtracts the 99th percentile (P_{99}) of the per grid cell–calculated wind support (high positive value, strong tailwinds), converting grid cells with strong tailwinds to zero and cells with headwinds to even higher negative values. In the following step, all cells are converted to cost (by taking their absolute values). Finally, all cells are standardised between zero and 100, by dividing with the parallel wind cost's 99th percentile and multiplying by 100: cells with low cost (close to zero Standardised Cost Units—SCU) are the ones that provide tailwinds, while those with high cost values (100 SCU) are the ones that exhibit headwinds (Figure 1a). If the LCPs were calculated using only this component, they would always follow the most favourable winds (highest wind support, see Figure 2a).

2.2.2 | 2nd Component: Standardised Crosswind Cost

The second component is the "standardised crosswind cost" (c_cost), which focuses on the axis perpendicular to the bird's movement and calculates the crosswind that a bird experiences when moving between two cells, resulting in movements with strong (high positive values), or weak (low positive values) crosswinds. Cells with low cost (close to zero SCU) are the ones that have weak crosswinds, while those with high cost values (close

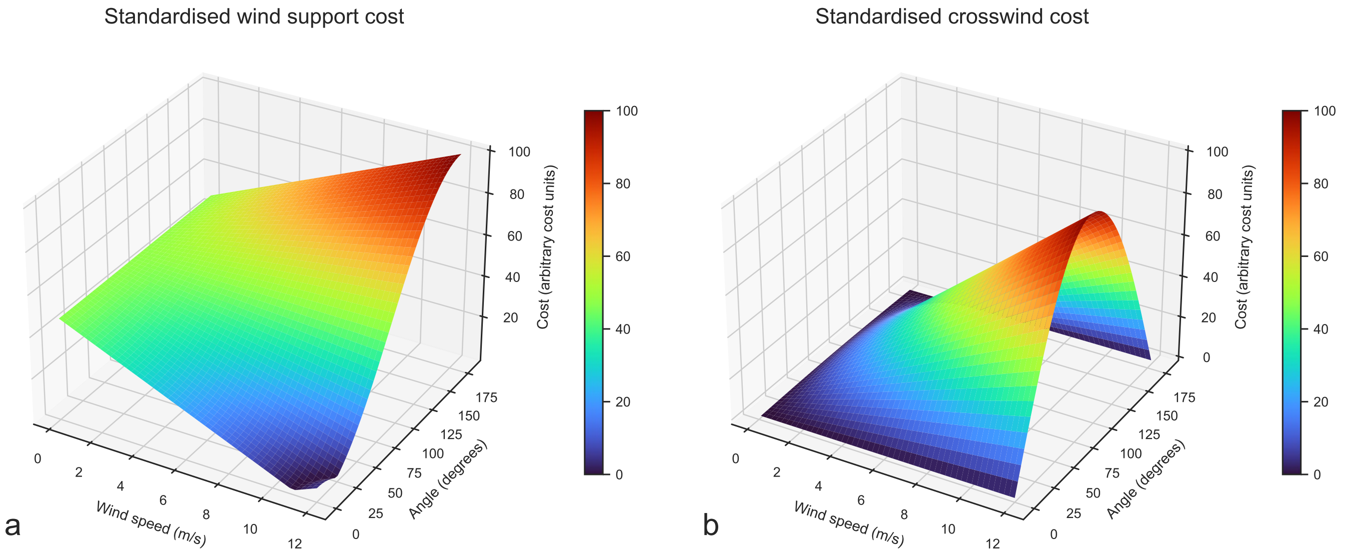

FIGURE 1 | (a) The range of the standardised parallel wind cost formula: Strong tailwinds (high wind speed combined with low angle between the bird's and the wind's direction) result in low cost (blue colour), while strong headwinds (high wind speed combined with high angle) result in high cost values (red colour). Every other wind-angle combination (weak tailwinds, weak headwinds, crosswinds) results in intermediate cost values (green colour). (b) The range of the standardised crosswind cost formula: Tailwinds and headwinds result in low cost, while strong crosswinds result in high cost values.

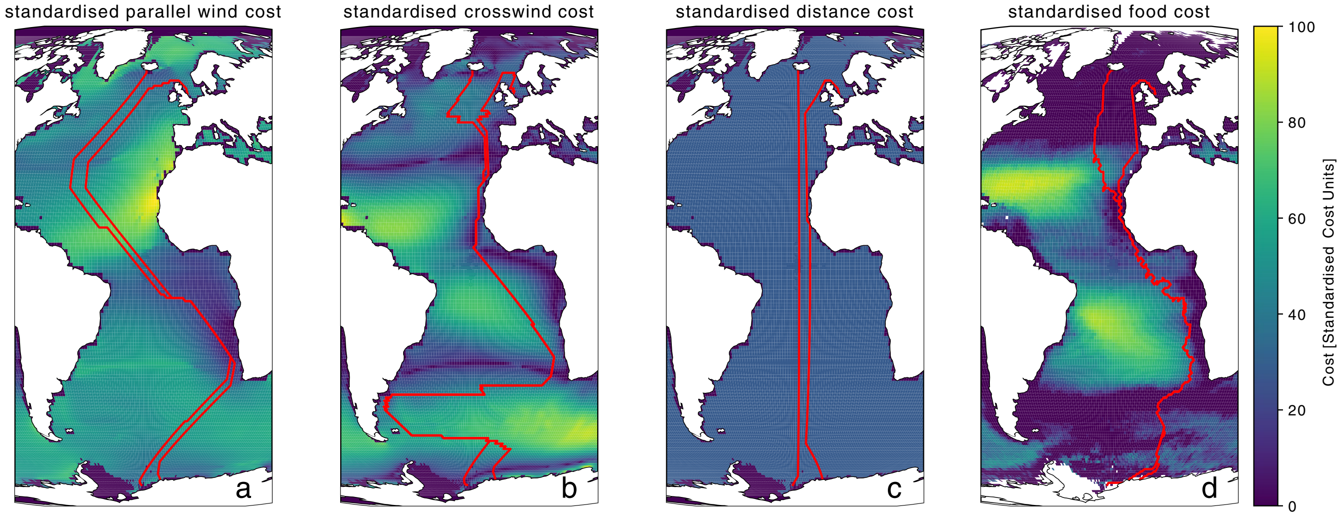

FIGURE 2 | Maps of cost (background colour) calculated using only (a) the first (parallel wind), (b) the second (crosswind), (c) the third (distance) and (d) the fourth (food) component of the complete cost formula. Cost per grid cell is calculated for a bird moving from South to North, and the red lines show the least cost path for each cost surface for birds migrating to Svalbard and to the Netherlands (tracks end in Iceland due to constant daylight limiting the accuracy of Geolocators). Projection used: Mollweide.

to 100 SCU) are the ones that have strong crosswinds (Figure 1b). If the LCP were to be calculated using only this component, then the path with the lowest cost would always be the one with the weakest perpendicular to the bird's direction winds (Figure 2b).

$$\text{crosswind cost}_{i,j} = |\vec{w}|_i \times sin\theta_{i,j}$$

$$\text{standardised cross wind cost}_{i,j} = \frac{100}{P_{99}(\text{crosswind cost})} \times \text{crosswind cost}_{i,j} \quad (3)$$

where $|\vec{w}|$: wind speed (magnitude of wind vector), i: the source cell, j: the target cell and θ: the angle between the wind vector ($\vec{w}$)and the bird's groundspeed ($\vec{g}$).

2.2.3 | 3rd Component: Standardised Distance Cost

The third component of the formula is the “standardised distance cost” (d_cost) or simply the cost defined as the number of grid cells (which of course depends on the resolution, i.e. the grid cell size) a bird has to travel between two locations, and is calculated using the following formula:

$$\text{standardised distance cost}_{i,j} = P_{50}(\text{standardised parallel wind cost}) \quad (4)$$

All grid cells of the cost surface take the same value: the median (P_{50}) of the w_cost Formula (2). With this method, birds get penalised by accumulating more cost when using a longer path. If the LCPs were calculated using only this component, then they would always take the shortest possible path (Figure 2c).

2.2.4 | 4th Component: Standardised Food Cost

The fourth component of the formula is the “standardised food cost” (f_cost), defined as the cost based on the availability of food for seabirds, using chl-a (chlorophyll a) as a proxy. A gridded chl-a remote sensing dataset is used as the cost surface, after applying a logarithmic transformation due to the positively skewed chl-a values. Following this transformation, all transformed values > −1 were replaced by −1. This approach converts all cells with an actual chl-a concentration over 0.1 mg/m^3 to cells with maximum values, that is, the most productive ocean areas. Finally, a value of 1 was added to all cells in order for the most productive grid cells to have a value of 0 (selected after performing a sensitivity analysis, see Figure S2), their absolute values were taken, and were standardised between zero and 100, resulting in highly productive areas having cost values close to zero SCU, and low-productivity areas having high cost values (close to 100 SCU).

$$\text{food cost}_{i,j} = \left|\log(\text{ch la})_i + 1\right|$$

$$\text{standardised food cost}_{i,j} = \frac{100}{P_{99}(\text{food cost})} \times \text{food cost}_{i,j} \quad (5)$$

where i: the source cell and j: the target cell.

If the LCPs were calculated using only this component, then birds would always follow the most productive path to the destination (Figure 2d).

2.3 | Combining All Components

Since birds most likely do not have a simplistic flight strategy (e.g., “always follow the tailwinds”) but rather a combination of strategies per location and per time of the year, even down to a subpopulation level, we use combinations of all four described components (see Formula (6)). Note that in this equation the final cost is simply based on linear relationships with the four cost components, as by lack of further knowledge we avoid making assumptions about the nature of these relationships, whereas in reality some might be non-linear and/or include thresholds (e.g., the food cost). The assigned weights (a, b, c, d) can take any value between 0 and 1 (for the w_cost and d_cost components) and between 0 and 0.5 for the c_cost and f_cost components. These thresholds were selected after performing a sensitivity analysis (Figure S3). During these tests, high values (over 0.5) for weights b (c_cost) and d (f_cost) yielded, in multiple cases, very long and unlikely flyways and improved the root mean square error (RMSE) of the simulations only marginally. The weights have been varied using an increment of 0.1 and their sum has to equal 1.0.

These simple rules result in a total number of 195 possible component combinations, yielding 195 different cost formulas and 195 cost surfaces with cost values per cell between 0 (minimum) and 100 SCU (maximum). Each of these surfaces has a unique LCP, and as a consequence, each simulation is repeated 195 times, producing 195 potential LCPs, each with its own unique weight combination. The rule requiring the sum of the weights to always equal one enhances the interpretability of the results, as each LCP corresponds to a unique combination of coefficients. If the sum were allowed to vary, we would need to analyse multiple LCPs with effectively the same coefficient ratios. For example, the combination a = 0.7 and b = 0.3 (sum = 1) is mathematically equivalent to a = 1.4 and $b = 0.6$ (sum = 2), leading to redundancy in the analysis.

$$cost_{i,j} = a \times \mathrm{w\_cost}_{i,j} + b \times \mathrm{c\_cost}_{i,j} + c \times \mathrm{d\_cost}_{i,j} + d \times \mathrm{f\_cost}_{i,j} \quad (6)$$

where w_cost: standardised parallel wind cost, c_cost: standardised crosswind cost, d_cost: standardised distance cost, f_cost: standardised food cost, and a, b, c and d: weights of the four cost components.

The RMSE was calculated as the square root of the mean squared distance (in km) between the simulated and the observed longitudinal position of the birds per 10° latitudinal bin.

$$\mathrm{RMSE} = \sqrt{\frac{\sum_{i=1}^{n} \left(\hat{y}_i - y_i\right)^2}{n}} \quad (7)$$

where $\hat{y}_i$: predicted longitudinal position along a LCP, y_i: observed longitudinal position of tagged birds, and n: number of positions along the flyway.

2.4 | The Environmental Data

Arctic terns typically migrate at low altitudes, near the water surface (Gudmundsson et al. 1992; Hedenström and Åkesson 2016); thus, we use the zonal (u10) and meridional (v10) surface wind components from the ECMWF Reanalysis v5 (ERA5) as actual wind conditions, at a spatial resolution of ~25 km and at an hourly temporal resolution. Six years of data (2012–2017) were used (Hersbach et al. 2023), averaged over seasons (winter: December–February, spring: March–May, summer: June–August, and autumn: September–November) and re-gridded to a spatial resolution of ~100 km (Schulzweida 2020). Running the model at a higher spatial resolution (25 km) produced similar results (Figure S4). Additionally, our intention is for our model to be compatible with ESM data in later studies, so we decided to use the average spatial resolution among Earth System Models (ESM): 100 km. Out of all four seasons, we use only the March–May and the September–November data for spring and autumn migration simulations, respectively, in order to cover the largest parts of the arctic tern migration periods (Egevang et al. 2010; Volkov et al. 2017). Finally, even though seabirds mostly use overwater routes, recent studies have revealed that several species (streaked shearwaters, arctic terns, common terns, sandwich terns and long-tailed skuas) in some cases use overland passages (Ward 2000; Wernham 2002; Wynn et al. 2014; Yoda et al. 2017; Lamb et al. 2018; Redfern and Bevan 2020). However, because overland passages are the exception, and since we believe that it is more important, as a first step, to fine-tune and evaluate the model's performance for the three fundamental factors (wind, food and distance), we decided to mask out land grid cells.

Following previous studies, we used Chlorophyll a (chl-a) as a proxy for seabird-related ocean productivity (Hromadkova et al. 2020; Morten et al. 2023). Seabirds do not consume phytoplankton directly but rather rely on large zooplankton and small fish (Egevang et al. 2010) which appear later in the same productive regions (Asch 2015; Suchy et al. 2022). We used chl-a data from the European Space Agency Ocean Colour Climate Change Initiative (ESA OC-CCI), version 5.0 dataset (Sathyendranath et al. 2019, 2021). The ESA OC-CCI program generates a set of validated essential climate variables from satellite observations. Six years of chl-a data (2012–2017) were used for the arctic terns, at a spatial resolution of 4 km and at a monthly temporal resolution. The data were then converted to the same spatiotemporal resolution as the ERA5 wind data (25 km). Since we are using seasonal means (3 months), a lag of a few weeks between phytoplankton growth and fish growth is not expected to introduce large uncertainties, so we assumed that chl-a can be used as a proxy for the productive ocean regions.

2.5 | Tracking Data

For the evaluation of the simulated flyways, we used bird tracking data from a total number of 72 arctic terns equipped with geolocators (for details see Skyllas et al. 2023), from two different populations: Svalbard ($n = 61$) and the Netherlands ($n = 11$). The median starting location of each population (median position of the first moving datapoint of the birds) was used as a starting point for all simulations. The median longitudinal position of each population was calculated per 10° of latitude and compared to the longitudinal position of each simulated flyway (195 in total, median per 10° lat). The 20 simulations with the lowest RMSE when compared to observations (tracking data) were selected as the top20 and were used for further analysis (Table 1 and Figure 4). An additional case study using three populations of sooty shearwaters (for details see Shaffer et al. 2006) is available in the Supporting Material (Figures S5–S8).

2.6 | Optimal Flyway Calculations

For each LCP, its length, median wind support, and median crosswind were evaluated. The length was calculated as the sum of the great circle distances between the consecutive points of each trajectory, while wind support and crosswind were determined using Formula (2) (wind support) and Formula (3) (crosswind cost).

TABLE 1 | Mean RMSE of the top20 simulations (simulated flyways with the lowest RMSE), and the number of simulations within 1σ from the minimum simulated flyway RMSE.

Migration	Top 20 Mean RMSE ±1 σ (km)	Simulations within 1σ from the minimum RMSE (number)	Simulations within 1σ from the minimum RMSE (%)
Svalbard spring	508 ± 19	60	31
Netherlands spring	334 ± 7	105	54
Svalbard autumn—America	667 ± 71	18	9
Svalbard autumn—Africa	937 ± 55	33	17
Netherlands autumn	529 ± 36	87	45

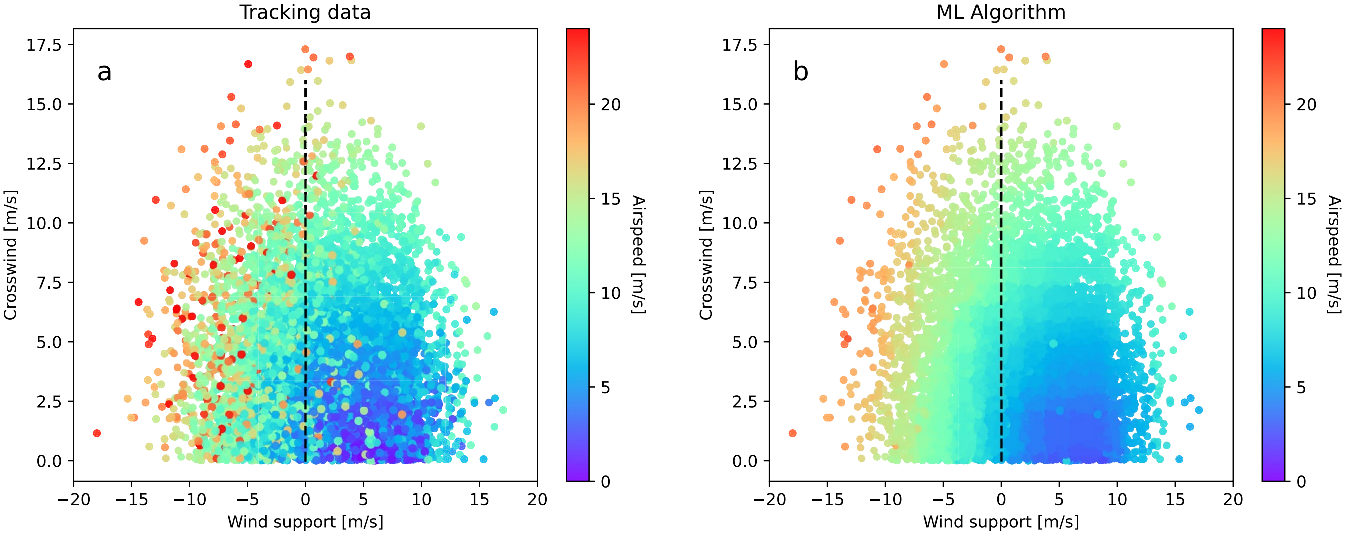

FIGURE 3 | Airspeed (colours) against wind support (*x*-axis) and crosswind (*y*-axis) for each arctic tern location (dots). The airspeed of the birds was (a) calculated using trigonometry on the GLS tracking data, with the wind conditions and the bird's groundspeed per location, while in (b) the airspeed was calculated by applying the trained ML algorithm on the wind conditions of the annotated tracking data.

A machine learning (ML) algorithm, gradient boosting regression, was trained on the arctic tern tracking data in order to infer the bird's airspeed (the speed of the animal relative to the air) from the prevailing wind conditions (wind support and crosswind, Figure 3a) and its location. Gradient boosting is a ML technique using an ensemble of weak prediction models, that is, models that make very few assumptions about the data, which are typically simple decision trees. This method is able to detect nonlinear relationships between the target (dependent) variable (airspeed) and the features (independent variables: wind support and crosswind). The goal was to fit the trained ML algorithm on the wind conditions of the simulated flyways (after annotating them) and predict an airspeed value for each location. Knowing the two sides of the triangle of velocities (McLaren et al. 2012; Hedenström and Åkesson 2016), and the angle between the groundspeed (speed of the animal relative to the ground) and wind vectors allowed for solving the third side of the triangle (groundspeed, Formula (9)).

$$\text{airspeed}_{i,j} = \sqrt{\text{groundspeed}_{i,j}^2 + |\vec{w}|_i^2 - 2 \times \text{groundspeed}_{i,j} \times |\vec{w}|_i \times (\cos\theta_{i,j})} \tag{8}$$

$$\text{groundspeed}_{i,j} = |\vec{w}|_i \times \cos\theta_{i,j} + \sqrt{\text{airspeed}_{i,j}^2 - |\vec{w}|_i^2 \times (\sin\theta_{i,j})^2} \tag{9}$$

where $|\vec{w}|$: wind speed (magnitude of wind vector), i: the source cell, j: the target cell and θ: the angle between the wind vector ($\vec{w}$) and the bird's groundspeed ($\vec{g}$).

Consequently, three more metrics were calculated for each of the 195 LCPs: the median airspeed, the duration (by summing the time needed for a simulated bird to cross a grid cell, as determined by the grid cell's dimensions and the bird's groundspeed, per LCP):

$$\text{duration} = \sum_{i=1}^{n-1} time_i \tag{10}$$

and finally, the total effort by summing the time-weighted airspeed at each grid cell, per LCP: grid cells with lower weights (less time for the simulated bird to cross the grid cell) contributed less to the total effort compared to grid cells with higher weights (more time for the simulated bird to cross the grid cell). Total effort is thus similar to the "total air distance", as used by Geisler et al. (2022), and has the same unit (km).

$$\text{total effort} = \sum_{i=1}^{n-1} \left(\text{airspeed}_i \times \text{time}_i\right) \tag{11}$$

Out of the 195 LCPs, a total number of 60 per migration (unique combination of population and season, for example: Netherlands spring), were selected for further analysis (Figure 4): the 10 LCPs each with (a) the highest median wind support, (b) lowest median crosswind, (c) highest median groundspeed, (d) shortest distance, (e) shortest duration and (f) lowest total effort. For visualisation purposes, each of these top10 groups of LCPs, were clustered using the algorithm from Adrienko and Andrienko (2011). This algorithm detects the "characteristic points" of the trajectories (start and end points, points of significant turns, and points of significant stops), and groups them based on spatial proximity. Then, for each pair of points, it aggregates the trajectory segments by counting the number of movements and computing the durations, lengths, and average speeds between the two points. This resulted in spatially generalised trajectories per cluster of top10 LCPs. The "shortest duration" cluster and the "lowest total effort" clusters are used as the "time optimising" and the "effort optimising" clusters from this point on, respectively. We refer to "effort minimisation" and not "energy minimisation", as the latter incorporates fuelling at non-breeding sites; we chose to omit the fuelling components of migration, including staging and wintering sites, to focus on the (flapping) flight component (see Alerstam and Lindström 1990).

3 | Results

Out of the 195 simulated flyways, we selected the 20 LCPs with the lowest RMSE compared to tracking data, in order to evaluate the effectiveness of our LCP method. The model succeeded in simulating almost all arctic tern flyways (Figure 5a–e), whether they follow wind circulation patterns by aligning with the prevailing westerlies in the mid latitudes and the easterlies in the lower latitudes and maximising wind support (Svalbard spring and Svalbard America autumn) or not (both Dutch migrations, and Svalbard Africa autumn). Our simulations closely follow the S-shaped flyway by the Svalbard birds in spring (RMSE ±1 $\sigma = 508 \pm 19$ km) as well as the straighter flyway of the Dutch population along the African coast (RMSE ±1 $\sigma = 334 \pm 7$ km). Similarly, the wind-supported autumn Svalbard migration along the American coastline, as well as the autumn Dutch migration along the African coastline, both yield comparable RMSE (667 ± 71 km and 529 ± 36 respectively). However, the autumn African flyway of the Svalbard population proves to be more challenging than the others, as the model fails to simulate the visit of the arctic terns to the North Atlantic staging site before continuing their southward journey. This discrepancy in the Northern Hemisphere results in an elevated RMSE (937 ± 55 km). However, when simulations were split into two parts with the North Atlantic staging area as an intermediate stop (Figure S10), the model was able to accurately simulate the entire flyway and generated at least 20 LCPs with low RMSE (311 and 616 km for the first and the second section, respectively).

Knowing how the observed flyways were simulated can lead to insights about the environmental factors responsible for each flyway's general shape. The two American flyways (Svalbard spring and Svalbard autumn—America), as hinted by their shape which follows the easterly trade winds in the lower latitudes and the westerlies in the mid latitudes, required a large contribution from the wind support component (median weight $a = 0.7$) signifying the reliance on wind circulation for arctic terns that opt for a tailwind-optimisation strategy. On the other hand, the African coast flyways require more complex strategies. All three of these (Netherlands spring, Netherlands autumn and Svalbard autumn—Africa) consist of a blend between crosswind minimisation, distance minimisation, and food optimisation (weights b, c and d, respectively), with weights for distance minimisation dominating (median values between 0.4 and 0.6). Interestingly, food appears to be more important in autumn (median weight $d = 0.3$) than in spring migrations (see also Figure S3).

Disentangling the complex interplay between wind conditions, a bird's efforts (airspeed) and the resulting groundspeed is necessary when addressing the issue of optimal migration. Practically, this means that the bird needs to exhibit a "specific flight behaviour" or, in other words, it needs to adjust its airspeed according to the prevailing wind conditions in a realistic way. For example, a bird might compensate for strong winds, resulting in

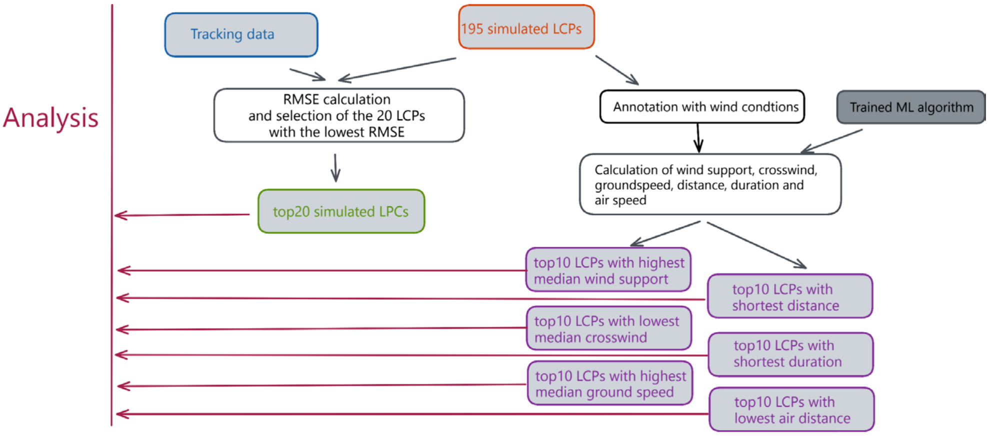

FIGURE 4 | Flowchart describing the main processing steps for the datasets used in this study.

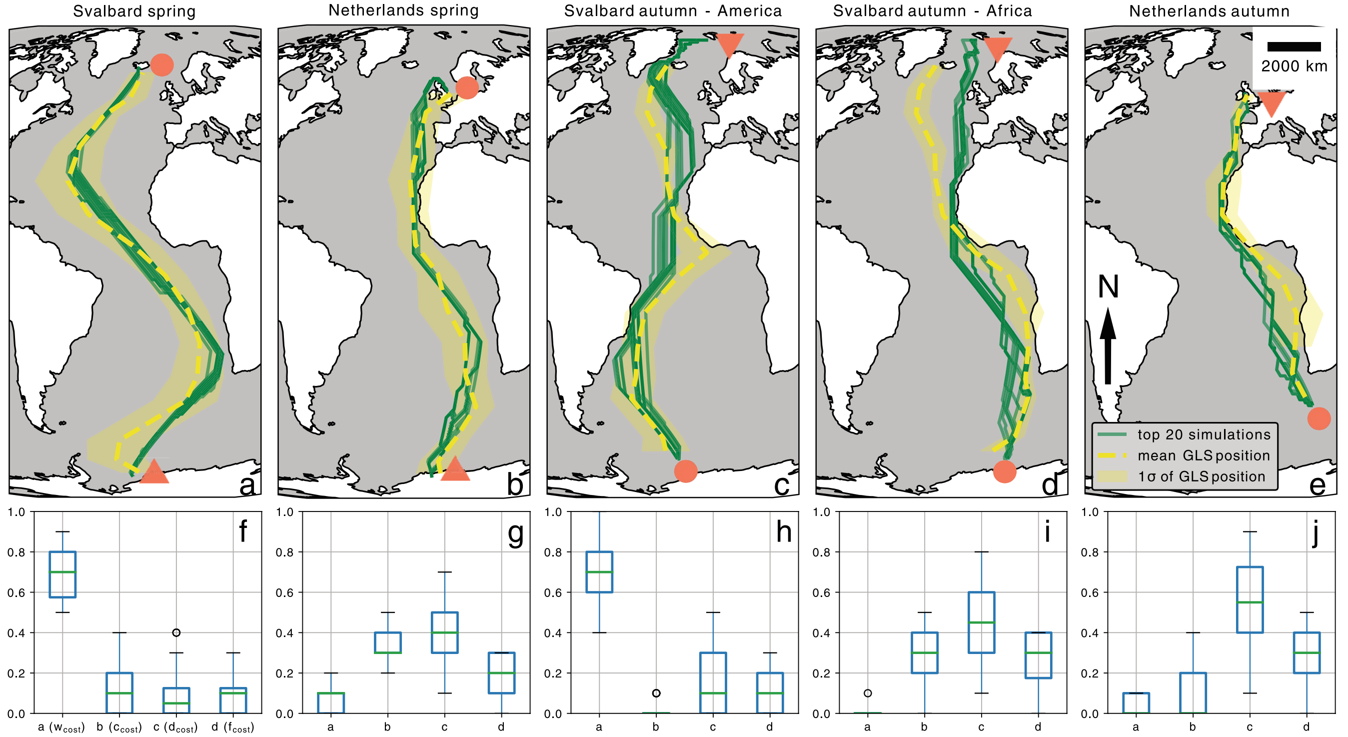

FIGURE 5 | The 20 simulated flyways with the lowest RMSE (green lines) for each arctic tern (a–e) migration, with their starting and ending regions marked by an orange triangle and an orange circle, respectively. The yellow lines depict the median longitudinal position of the tracking data per 10° of latitude, with the yellow shade showing the ±1σ. The second row contains box plots with the combination of weights (*x*-axis) that yielded the top20 simulations (f–j). Projection used: Mollweide.

a high airspeed value. We approached this challenge by training a machine learning algorithm on the arctic tern tracking data. More specifically, we used the bird's wind conditions (wind support and crosswind experienced by the bird) to predict its airspeed, which resulted in an ML model with wind support and crosswinds having relative importances of 65% and 35% respectively. Moreover, we trained a second model using additional features: the bird's population (Svalbard or Netherlands), season, position (longitude and latitude) and wind conditions (wind support and crosswind) from our tracking data. This resulted in an ML model with three dominant features: wind support (relative importance for the ML algorithm: 59.2%), crosswind (31.3%) and latitude (7.9%), indicating that the arctic terns' airspeed depended mainly on the wind, but also on the latitude that the bird was at (Figure S11). However, since the addition of longitude and latitude as features could lead to an overfitting of the model for the specific birds (arctic terns) flying over the AO, we decided to use the first, more general model, including only wind support and crosswind. This, more general model, captured the general pattern of the arctic terns' "specific flight behaviour" reasonably well (Figure 3a,b, RMSE = 2.96 m/s, $R^2 = 0.6$).

Using the ML—derived airspeeds, we were able to calculate the simulated LCPs offering time- or effort-optimisation (migrations with the shortest durations and the lowest total efforts, respectively). During the two wind-supported migrations (Svalbard spring and Svalbard autumn—America), the arctic terns follow closely (RMSE = 527 km) the minimum total effort cluster (Figure 6a,c) which overlaps largely with the wind support and groundspeed maximisation clusters. Even though these effort-minimising flyways are longer (in distance) than the time-minimising flyways (19,138 km vs. 16,332 km for Svalbard spring and 18,228 km vs. 16,477 km for Svalbard autumn—America), they offer lower effort expenditure (13,364 km vs. 17,592 km for Svalbard spring and 16,322 km vs. 18,710 km for Svalbard autumn—America) and higher groundspeeds (26.8 km/h vs. 24.8 km/h and 25.4 km/h vs. 24.7 km/h). Higher groundspeeds, practically, mean that the effort-minimising flyways only last a few days longer (28.7 vs. 26.5 days and 29.1 vs. 27.4 days) than the time-minimising ones. The spring migration of the Dutch arctic terns is interesting (Figure 6b) since it seems to combine the best of both worlds: in the Southern Hemisphere they opt for a flyway that is not much longer than the shortest one (19,157 km) but offers higher wind support and groundspeed, combined with low crosswinds. At the same time, the aforementioned advantages translate to time- and effort-minimising clusters being very close to each other, allowing the birds to travel fast and efficiently. It is in the Northern Hemisphere where they are faced with a decision: follow the (much longer) effort-optimising flyway or the (shorter) time-optimising one? In this part of the Atlantic Ocean they eventually stay close to the African coast, expend more effort than the effort-minimising cluster (22,207 km vs. 18,524 km), face the headwinds, and still manage to complete a shorter trip (34.2 days vs. 35.2 days).

In the two autumn migrations along the African coast, the wind support and groundspeed maximising clusters (Svalbard autumn—Africa: 25,679 and 25,728 km, Netherlands autumn: 22,120 and 22,175 km, see Figure 6d,e) are much longer than the shortest ones (Svalbard autumn—Africa: 17,383 km, Netherlands autumn: 13,250 km). It is this difference that results in optimal time and effort flyways largely overlapping and being close to the shortest routes. No matter how low the mean

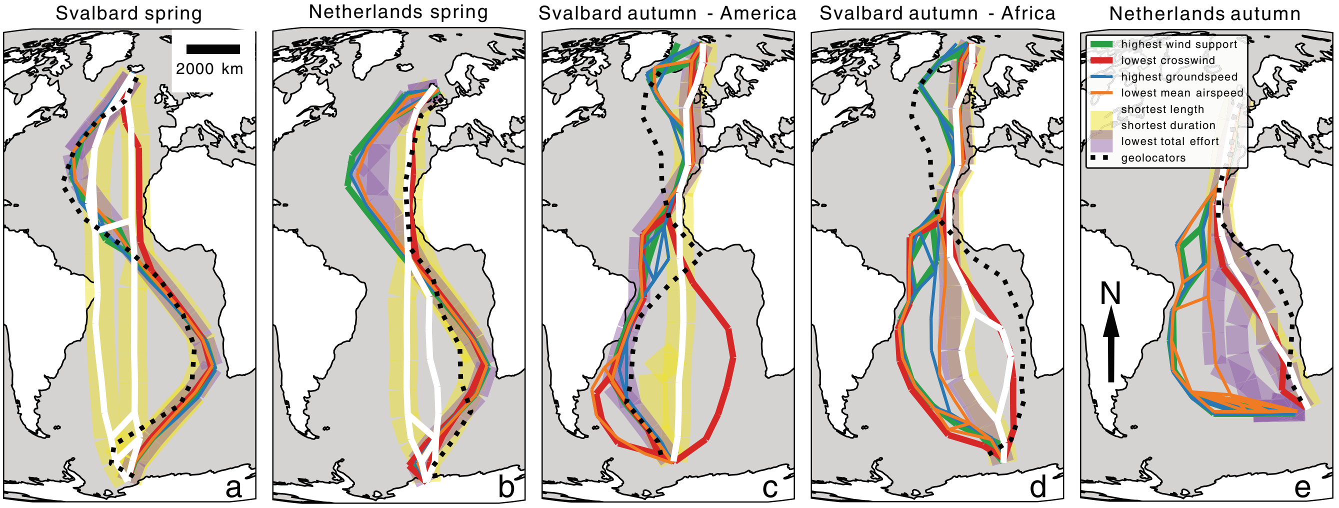

FIGURE 6 | Top10 simulated flyways for each of the seven optimisation strategies: Highest wind support, lowest crosswind, lowest airspeed, highest groundspeed, shortest length, shortest duration and lowest total effort, for each of the seven migrations (unique population and season combinations). The top10 flyways are depicted as clusters for clearer visualisation. Airspeeds are calculated from wind support and crosswind using the trained ML algorithm, groundspeeds using the law of cosines. The median longitudinal position of the tracking data (black dotted line) is plotted for reference. Projection used: Mollweide.

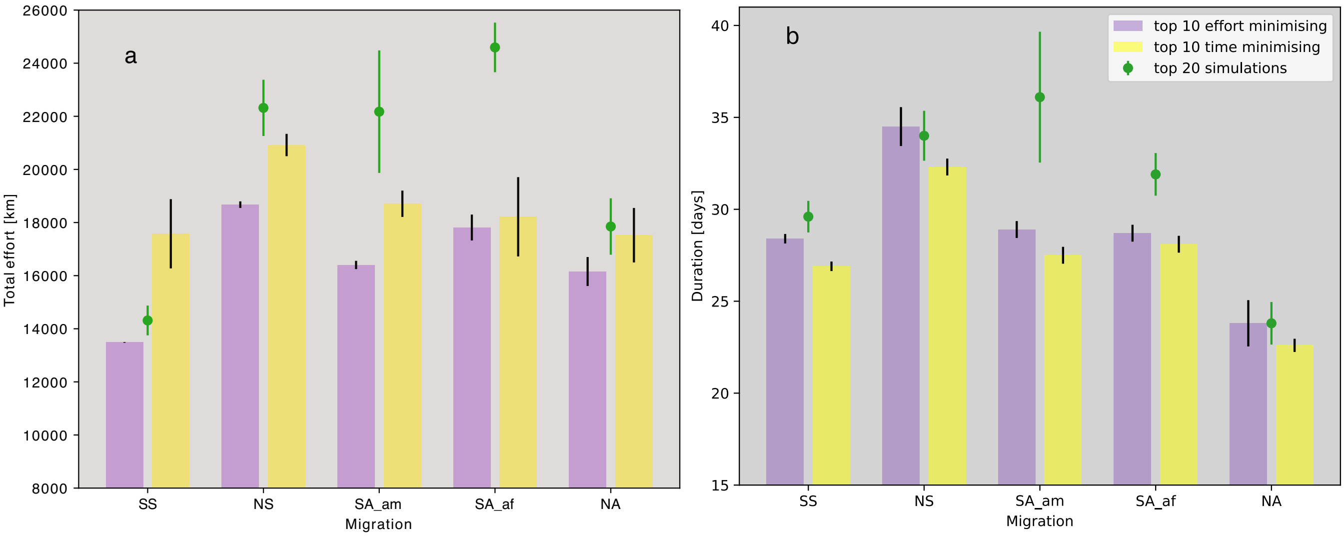

FIGURE 7 | (a) Mean total effort (km) for the arctic terns ±1σ (error bars) of the top20 simulations (green dots, lowest RMSE when compared to observations), of the top10 effort-minimising simulations (purple bars) and of the top10 time-minimising simulations (yellow bars), per migration (*x*-axis). (b) Depicts the same, only for duration ±1σ (days). The purple and yellow bars can be seen as theoretical limits (in terms of effort and duration) of the two opposite strategies: Effort and time minimisation. The green dots are closer to the truth (depending on how well we simulated the actual flyways) and depict what the birds actually do.

effort is in the wind-optimised clusters, they are still too long, resulting in elevated total effort values and forcing the time- and effort-optimising solutions to be shorter alternatives. In both cases, however, the actual tracking data deviate from the time- and effort-optimising clusters (but are captured by our top20 simulations) and follow closely the African coast and potentially the productive ocean regions, which could further improve the energy balance of the effort-optimising clusters by increasing the energy input. In Svalbard autumn—Africa, both optimal clusters overlap in large parts with the shortest distance cluster. Following the wind circulation (high wind support and groundspeed) would require the birds to deviate so much from their preferred direction of movement that it would result in very high total effort. Due to the position of their starting and end locations, it makes sense in terms of effort and time to simply follow the African coast, which also provides feeding opportunities and low crosswinds (Skyllas et al. 2023).

We then compared the actual strategies of the birds (using our top20 simulations) to the effort and time-minimisation strategies. More specifically, the top20 Svalbard spring simulations have a mean total effort value and a duration close to that of the effort optimisation cluster, confirming what is shown in Figure 6: the Svalbard birds select an effort-optimising strategy during the spring migration (Figure 7a,b). The Dutch spring migration, on the other hand, is closer to the mean effort of the time-optimising cluster but higher than the mean duration of this cluster. This is most likely due to the deviation (between the actual flyway and the time-minimising cluster, Figure 6b) in the Southern Hemisphere, and not because the birds follow an effort-minimising strategy. As a result, the Dutch arctic terns expend 56.4% more effort compared to Svalbard spring (22,207 ± 1099 km vs. 14,199 ± 559 km) and arrive almost 4 days (12.3%) earlier at their breeding grounds (34.2 ± 1.3 days vs. 30 ± 0.9 days). Svalbard autumn—America was expected to be closer to the effort-optimising cluster values (16,322 km and 29.1 days) but instead, the arctic terns actually spend 21,067 km (29.1% more effort) and 36.4 days (25.1% longer), probably due to the detour to the North Atlantic staging site, which is captured successfully by our top20 simulations (Figure 5c). However, the rewards of the staging site potentially offset these sacrifices.

Both autumn African flyways (Netherlands autumn and Svalbard autumn—Africa) have largely overlapping time- and effort-optimising clusters (Figure 6d,e). This can also be seen in Figure 7, with theoretical limits (mean values of the effort and time optimisation clusters) being close and offering little room for intermediate strategies. Capturing the Dutch birds' flyway well (Netherlands spring, Figure 5e) leads to mean effort and time values exactly as expected (Figure 7). However, the flyway followed by the Svalbard birds (Svalbard autumn—Africa) is neither effort- nor time-optimised. It is definitely short and grants weak crosswinds, but in no case does it follow the longer, more time- and effort-efficient clusters, resulting in higher total effort and duration values (24,541 km and 31.9 days) than theoretically expected (17,792 and 18,227 km, 28.9 and 28.2 days). This strategy seems to sacrifice time and energy, but as with the Dutch population, it can potentially offer other advantages such as food (both in the North Atlantic staging site and in the African coast) and easier navigation (Skyllas et al. 2023) changing the total energy budget of this migration and rewarding their effort and time sacrifices.

4 | Discussion

Based on a cost function that combines a limited number of environmental variables, we accurately simulated flyways of different shapes, lengths, and durations across both the Atlantic and Pacific Oceans. We show that these different flyways are the result of variable environmental conditions and different population-specific behaviours. For example, the characteristic S-shape of the Svalbard arctic terns results from following the westerlies and the trade winds, whereas the absence of this shape in the Dutch arctic terns results from flying against these same winds. We also show that these population-specific behaviours lead to effort minimisation in one population (Svalbard) and to time minimisation in the other (Dutch)—differences that are most likely related to a population-specific context that determines survival and reproduction. Overall, we accomplish this with a simple cost framework that can be expanded and adapted in future research to include more complexity and species. Our results demonstrate that Earth's environmental and physical properties underlie the global distribution of the migratory bird species used in our study and therefore need to be considered in studies that evaluate the long-range movement patterns and distribution of migratory birds.

The formation of flyways can be studied from observation-to-simulation, but also from simulation-to-observation (Beatty 1994; Laland et al. 2011; Dickins and Barton 2013). A simulation-to-observation approach like ours focuses on "how" flyways are created by combining environmental conditions without underlying assumptions. This results in a suite of climatically feasible flyways, each with different advantages; while one maximises groundspeed, another minimises crosswinds, and so forth. These climate-derived flyways can then be compared with observed tracks, illuminating how the interactions between climate and a bird's goals form the flyways that exist in nature. This differs from the more usual observation-to-simulation approach of tracking individual birds and then trying to understand the resulting tracks.

Even when a model is in its early stages and validated with only limited datasets, it can still offer valuable insights (see sooty shearwater case study, Figures S5–S8). In our case, the 195 climatically feasible flyways are based on simple, fundamental rules: they optimise wind, distance, and food availability, showing what is "climatically feasible" for a bird to do. Moreover, these flyways tend to cluster (see Supporting Material, Figures S4 and S9), with each cluster optimising similar objectives. These clusters provide a rough estimate of the range within which bird observations, such as mean tracking positions, may fall. Additionally, the 195 climatically feasible flyways can be annotated with wind conditions and airspeed (as demonstrated in our study) to visualise alternative hypothetical flyways that seabirds might follow between two locations if they were to optimise different objectives, such as time, effort, or wind support (as seen in the top10 clusters in our study). We argue, therefore, that even with limited validation, this approach offers a preliminary guideline for how flyways may be shaped and positioned based on environmental conditions, while also suggesting potential alternatives.

As our model continues to be refined and validated with additional tracking data across various species and regions, its predictive capabilities are likely to improve. Eventually, it may even allow for future flyway predictions without requiring extensive tracking data. This would enable researchers to study how birds' distribution and movement patterns are influenced by environmental variables, and how these patterns might shift due to climate change (La Sorte et al. 2019; Somveille et al. 2020; Morten et al. 2023; Skyllas et al. 2023)—an essential insight for designing effective climate mitigation strategies. A refined and well-validated model could provide insights into the temporal and spatial distribution of birds without needing to track large numbers of individuals. Moreover, this simulation-to-observation model could serve as a tool for generating a priori hypotheses about time and effort minimisation before tracking begins, suggesting strategies that have not yet been observed. In climate science, multiple models are often used to provide an "ensemble mean" and a measure of uncertainty, known as "model spread." Similar approaches are common in machine learning. The application of multiple "flyway models" would be similarly beneficial, allowing us to quantify uncertainty and make more robust predictions. Efforts like the development of the Revell and

Somveille (2017) model are invaluable in this regard. We agree with their statement: "Without causal understanding, it is not possible to make reliable predictions for populations that have not yet been tracked, or for future movement patterns under environmental change" (Revell and Somveille 2017), and we would add one small amendment: "Without causal understanding and multiple, independently developed models…".

To determine whether the observed behaviour minimises time or effort, the alternatives need to be simulated by making assumptions about different factors, for example, direction, airspeed and groundspeed. A common approach is to assume a constant airspeed (see Kranstauber et al. 2015; Loonstra et al. 2019; Morten et al. 2023), use that value to calculate important parameters such as trip duration and groundspeed, and later identify time- and effort-optimised clusters. We believe that making such assumptions can obscure valuable information. For example, assuming a constant airspeed yields an effort-minimisation cluster that is identical to the distance-minimisation cluster, since the cumulative effort expended by a bird depends on distance and daily effort (Figure S12). Similarly, assuming a constant groundspeed yields a time-minimisation cluster that is the same as the distance-minimisation cluster; if groundspeed is constant, it has no influence on the duration of the journey, so only distance determines its duration (Figure S13). To disentangle this 'triangle of velocities', that is, groundspeed, airspeed and wind support, we used a machine learning algorithm that factored in both wind support and crosswind to estimate airspeed (Shamoun-Baranes et al. 2007). One notable finding was a considerable effect of latitude on airspeed. We hypothesise that this effect stems from latitude being a proxy for how far along arctic terns are in their journey; it is possible for a bird's strategy to change during migration as its short-term objectives change (Vansteelant et al. 2017; Skyllas et al. 2023), and latitude could be a reflection of this change.

Our model allows us to evaluate the differing impacts of multiple environmental variables on migrating birds. Although this is an advance compared to earlier models that only included wind support or food availability, there is still room for improvement. For one, our model assumes that the impact (weight) of each environmental variable is constant from start to finish, but it is likely that their relative impacts, that is, in combination with a bird's objectives, will change throughout the migration or between years. Food availability, for example, will become more of a priority when a bird's fuel reserves are low. In addition, our model currently only allows linear relationships between the cost (y) and the four environmental variables (x), but some of these relationships might be non-linear in reality, for example, when more food does not lower the cost, because there is ample food already.

We have focused on the large spatiotemporal patterns of a seabird species, and our framework likely needs to be expanded or adapted in order to apply it to other purposes and questions. For example, future researchers might consider incorporating additional environmental variables, such as pressure, temperature, and convection (Shamoun-Baranes et al. 2010). Another option would be to allow birds to adjust their flight altitude (Loonstra et al. 2019) by expanding the number of neighbouring cells from eight, as used in this study's two-dimensional cost surface, to 24. This would include eight cells above and eight below the current altitude layer of the bird. Additionally, a new cost metric could be introduced to account for the wind's effect during these altitude changes. These changes could easily be implemented within the same framework. Future researchers may also want to use our model for different purposes, for example, to explain individual variation between individual birds or seasonal variation. Similarly, using daily or weekly environmental data instead of seasonal data would enable a more detailed assessment of the consequences of temporal variation. A more technical adjustment that might be necessary for broader use is adopting a hexagonal grid (instead of using a rectangular grid as employed here). This idea stems from our model's oversensitivity to the initial location of the shearwater population that winters in Japan (Figure S5d), which we believe is because this location is between two atmospheric circulation cells, and the extended zonal movement of this population at such high latitude tests the limits of models that use square grids. In a hexagonal grid, no additional corrections for the grid cell area need to be applied, since all hexagon cells have identical dimensions.

We focus solely on analysing time- and effort-minimisation paths and omit risk minimisation, even though this is also an important component of optimal migration theory. This omission is because we were unable to devise a simple but effective predation-risk proxy from environmental variables (but see McCabe et al. 2018, where risk is defined more broadly, and several mortality factors are combined). It should also be noted that we always refer to "effort minimisation" and not "energy minimisation." The latter, which is used in optimal migration theory, incorporates fuelling at non-breeding sites; we chose to omit the fuelling components of migration, including staging and wintering sites, to focus on the (flapping) flight component (see Alerstam and Lindström 1990). Most arctic terns probably forage on the wing, so from our tracking data we neither observed nor studied stopovers. However, including stopover sites and accumulation rates, that is, the fuelling component of migration, would give a more complete picture (see Alerstam and Lindström 1990). It is also important to note that to really understand 'why' a flyway is optimal, we would need to know how minimising time or energy impacts a bird's reproduction and survival. This underlines the need for tracking studies that simultaneously document mortality and reproduction, which are currently lacking.

Author Contributions

Nomikos Skyllas: conceptualisation, methodology, validation, formal analysis, investigation, data curation, writing – original draft, writing – review and editing, visualisation, project administration. **Mo A. Verhoeven:** conceptualisation, investigation, resources, writing – original draft, writing – review and editing, supervision, project administration. **Maarten J. J. E. Loonen:** resources, supervision; **Richard Bintanja:** resources, supervision, funding acquisition.

Acknowledgements

We would like to thank Bart A. Nolet for engaging in lengthy discussions and providing insightful feedback. His contributions greatly influenced the development of this manuscript. We express our gratitude to the Department of Theoretical and Computational Ecology (TCE) of the Institute for Biodiversity and Ecosystem Dynamics (IBED) in the University of Amsterdam (UvA); The presentations delivered during the departmental meetings, along with the discussions with its members, proved highly beneficial and sparked fresh ideas. We extend our gratitude to Scott A. Shaffer and David R. Thompson for sharing the Pacific Ocean Sooty Shearwater data, which enriched our study by highlighting further applications of our method. We also thank Fiona Smith for providing the geolocator data from the two Arctic tern populations. Geolocators were financed through crowd-funding by the Ubbo Emmius fund among alumni of the University of Groningen. Many people helped with equipping and retrieving geolocators. In The Netherlands, Derrick Hiemstra played an essential role as leader of the tern ringing project. Petra Manche assisted both on Svalbard and in The Netherlands, and Suzanne Lubbe assisted several years as a volunteer on Svalbard. Many students helped locate and catch the terns. On Svalbard: Tim van Oosten, Malenthe Teunis, Hannah van Noort, Jan-Willem Loonen, Willemijn Loonen, Fiona Smith, Anne Schumacher, Mari Fjelldal, and Kristle Kranenburg. In The Netherlands, Gerben Krosschell and Thomas Zaw assisted in fieldwork and analysing data.

Conflicts of Interest

The authors declare no conflicts of interest.

Data Availability Statement

The data supporting the results in this paper are available at Zenodo: https://doi.org/10.5281/zenodo.14825746.*Code Availability*: The scripts supporting the results in this paper are available at Zenodo: https://doi.org/10.5281/zenodo.14825789.

References

Adrienko, N., and G. Andrienko. 2011. "Spatial Generalization and Aggregation of Massive Movement Data." *IEEE Transactions on Visualization and Computer Graphics* 17, no. 2: 205–219. https://doi.org/10.1109/TVCG.2010.44.

Alerstam, T., and Å. Lindström. 1990. "Optimal Bird Migration: The Relative Importance of Time, Energy, and Safety." In *Bird Migration: Physiology and Ecophysiology*, edited by E. Gwinner, 331–351. Springer.

Asch, R. G. 2015. "Climate Change and Decadal Shifts in the Phenology of Larval Fishes in the California Current Ecosystem." *Proceedings of the National Academy of Sciences of the United States of America* 112, no. 30: E4065–E4074. https://doi.org/10.1073/pnas.1421946112.

Beatty, J. 1994. "The Proximate/Ultimate Distinction in the Multiple Careers of Ernst Mayr." *Biology & Philosophy* 9, no. 3: 333–356. https://doi.org/10.1007/BF00857940.

Boere, G., C. A. Galbraith, and D. A. Stroud. 2006. *Waterbirds Around The World: A Global Overview of the Conservation, Management and Research of the world's Waterbird Flyways*. Stationery Office.

Dickins, T. E., and R. A. Barton. 2013. "Reciprocal Causation and the Proximate-Ultimate Distinction." *Biology and Philosophy* 28, no. 5: 747–756. https://doi.org/10.1007/s10539-012-9345-z.

Dijkstra, E. W. 1959. "A Note on Two Problems in Connexion With Graphs." *Numerische Mathematik* 1: 269–271. https://doi.org/10.1007/BF01386390.

Egevang, C., I. J. Stenhouse, R. A. Phillips, A. Petersen, J. W. Fox, and J. R. D. Silk. 2010. "Tracking of Arctic Terns *Sterna Paradisaea* Reveals Longest Animal Migration." *Proceedings of the National Academy of Sciences of the United States of America* 107, no. 5: 2078–2081. https://doi.org/10.1073/pnas.0909493107.

Felicísimo, Á. M., J. Muñoz, and J. González-Solis. 2008. "Ocean Surface Winds Drive Dynamics of Transoceanic Aerial Movements." *PLoS One* 3, no. 8: 1–7. https://doi.org/10.1371/journal.pone.0002928.

Fernández-López, J., and K. Schliep. 2019. "rWind: Download, Edit and Include Wind Data in Ecological and Evolutionary Analysis." *Ecography* 42, no. 4: 804–810. https://doi.org/10.1111/ecog.03730.

Geisler, J., J. Madsen, B. A. Nolet, and K. H. T. Schreven. 2022. "Sea Crossings of Migratory Pink-Footed Geese: Seasonal Effects of Winds on Flying and Stopping Behaviour." *Journal of Avian Biology* 2022, no. 10: 1–16. https://doi.org/10.1111/jav.02985.

González-Solís, J., A. Felicísimo, J. W. Fox, V. Afanasyev, Y. Kolbeinsson, and J. Muñoz. 2009. "Influence of Sea Surface Winds on Shearwater Migration Detours." *Marine Ecology Progress Series* 391: 221–230. https://doi.org/10.3354/meps08128.

Gudmundsson, G. A., T. Alerstam, and B. Larsson. 1992. "Radar Observations of Northbound Migration of the Arctic Tern, *Sterna Paradisaea*, at the Antarctic Peninsula." *Antarctic Science* 4, no. 2: 163–170. https://doi.org/10.1017/S0954102092000257.

Hedenström, A., and S. Åkesson. 2016. "Ecology of Tern Flight in Relation to Wind, Topography and Aerodynamic Theory." *Philosophical Transactions of the Royal Society, B: Biological Sciences* 371, no. 1704: 20150396. https://doi.org/10.1098/rstb.2015.0396.

Hersbach, H., B. Bell, P. Berrisford, et al. 2023. "ERA5 Hourly Data on Single Levels From 1940 to Present." Copernicus Climate Change Service (C3S) Climate Data Store (CDS). https://doi.org/10.24381/cds.adbb2d47.

Hromadkova, T., V. Pavel, J. Flousek, and M. Briedis. 2020. "Seasonally Specific Responses to Wind Patterns and Ocean Productivity Facilitate the Longest Animal Migration on Earth." *Marine Ecology* 638: 1–12. https://doi.org/10.3354/meps13274.

Kranstauber, B., R. Weinzierl, M. Wikelski, and K. Safi. 2015. "Global Aerial Flyways Allow Efficient Travelling." *Ecology Letters* 18, no. 12: 1338–1345. https://doi.org/10.1111/ele.12528.

La Sorte, F. A., K. G. Horton, C. Nilsson, and A. M. Dokter. 2019. "Projected Changes in Wind Assistance Under Climate Change for Nocturnally Migrating Bird Populations." *Global Change Biology* 25, no. 2: 589–601. https://doi.org/10.1111/gcb.14531.

Laland, K. N., K. Sterelny, J. Odling-Smee, W. Hoppitt, and T. Uller. 2011. "Cause and Effect in Biology Revisited: Is Mayr's Proximate-Ultimate Dichotomy Still Useful?" *Science* 334, no. 6062: 1512–1516. https://doi.org/10.1126/science.1210879.

Lamb, J. S., D. J. Newstead, L. M. Koczur, B. M. Ballard, M. C. Green, and P. G. R. Jodice. 2018. "A Bridge Between Oceans: Overland Migration of Marine Birds in a Wind Energy Corridor." *Journal of Avian Biology* 49, no. 2: jav-01474. https://doi.org/10.1111/jav.01474.

Lisovski, S., R. Neumann, T. Albrecht, et al. 2021. "The Indo-European Flyway: Opportunities and Constraints Reflected by Common Rosefinches Breeding Across Europe." *Journal of Biogeography* 48, no. 6: 1255–1266. https://doi.org/10.1111/jbi.14085.

Loonstra, A. H. J., M. A. Verhoeven, N. R. Senner, C. Both, and T. Piersma. 2019. "Adverse Wind Conditions During Northward Sahara Crossings Increase the In-Flight Mortality of Black-Tailed Godwits." *Ecology Letters* 22, no. 12: 2060–2066. https://doi.org/10.1111/ele.13387.

McCabe, J. D., B. J. Olsen, B. Osti, and P. O. Koons. 2018. "The Influence of Wind Selectivity on Migratory Behavioral Strategies." *Behavioral Ecology* 29, no. 1: 160–168. https://doi.org/10.1093/beheco/arx141.

McLaren, J. D., J. Shamoun-Baranes, and W. Bouten. 2012. "Wind Selectivity and Partial Compensation for Wind Drift Among Nocturnally Migrating Passerines." *Behavioral Ecology* 23, no. 5: 1089–1101. https://doi.org/10.1093/beheco/ars078.

Morten, J. M., P. J. Buchanan, C. Egevang, et al. 2023. "Global Warming And Arctic Terns: Estimating Climate Change Impacts on the world's Longest Migration." *Global Change Biology* 29, no. 19: 5596–5614. https://doi.org/10.1111/gcb.16891.

Muñoz, J., Á. M. Felicísimo, F. Cabezas, A. R. Burgaz, and I. Martínez. 2004. "Wind as a Long-Distance Dispersal Vehicle in the Southern Hemisphere." *Science* 304, no. 5674: 1144–1147. https://doi.org/10.1126/science.1095210.

Norevik, G., S. Åkesson, T. Artois, et al. 2019. “Wind-Associated Detours Promote Seasonal Migratory Connectivity in a Flapping Flying Long-Distance Avian Migrant.” *Journal of Animal Ecology* 89, no. 2: 635–646. https://doi.org/10.1111/1365-2656.13112.

Prop, J., J. M. Black, and P. Shimmings. 2003. “Travel Schedules to the High Arctic: Barnacle Geese Trade-Off the Timing of Migration With Accumulation of Fat Deposits.” *Oikos* 103, no. 2: 403–414. https://doi.org/10.1034/j.1600-0706.2003.12042.x.

Rakhimberdiev, E., S. Duijns, J. Karagicheva, et al. 2018. “Fuelling Conditions at Staging Sites Can Mitigate Arctic Warming Effects in a Migratory Bird.” *Nature Communications* 9, no. 1: 1–10. https://doi.org/10.1038/s41467-018-06673-5.

Redfern, C. P. F., and R. M. Bevan. 2020. “Use of Sea Ice by Arctic Terns *Sterna Paradisaea* in Antarctica and Impacts of Climate Change.” *Journal of Avian Biology* 51, no. 2: 1–12. https://doi.org/10.1111/jav.02318.

Revell, C., and M. Somveille. 2017. “A Physics-Inspired Mechanistic Model of Migratory Movement Patterns in Birds.” *Scientific Reports* 7, no. 1: 1–10. https://doi.org/10.1038/s41598-017-09270-6.

Safi, K., B. Kranstauber, R. Weinzierl, et al. 2013. “Flying With the Wind: Scale Dependency of Speed and Direction Measurements in Modelling Wind Support in Avian Flight.” *Movement Ecology* 1, no. 1: 1–13. https://doi.org/10.1186/2051-3933-1-4.

Sathyendranath, S., R. J. W. Brewin, C. Brockmann, et al. 2019. “An Ocean-Colour Time Series for Use in Climate Studies: The Experience of the Ocean-Colour Climate Change Initiative (OC-CCI).” *Sensors* 19: 4285. https://doi.org/10.3390/s19194285.

Sathyendranath, S., T. Jackson, C. Brockmann, et al. 2021. “ESA Ocean Colour Climate Change Initiative (Ocean_Colour_cci): Version 5.0 Data.” NERC EDS Centre for Environmental Data Analysis, 19 May 2021. https://doi.org/10.5285/1dbe7a109c0244aaad713e078fd3059a.

Schulzweida, U. 2020. CDO User Guide (2.0.0) Zenodo. https://doi.org/10.5281/zenodo.5614769.

Shaffer, S. A., Y. Tremblay, H. Weimerskirch, et al. 2006. “Migratory Shearwaters Integrate Oceanic Resources Across the Pacific Ocean in an Endless Summer.” *Proceedings of the National Academy of Sciences of the United States of America* 103, no. 34: 12799–12802. https://doi.org/10.1073/pnas.0603715103.

Shamoun-Baranes, J., E. Van Loon, F. Liechti, and W. Bouten. 2007. “Analyzing the Effect of Wind on Flight: Pitfalls and Solutions.” *Journal of Experimental Biology* 210, no. 1: 82–90. https://doi.org/10.1242/jeb.02612.

Shamoun-Baranes, J., W. Bouten, and E. E. Van Loon. 2010. “Integrating Meteorology Into Research on Migration.” *Integrative and Comparative Biology* 50, no. 3: 280–292. https://doi.org/10.1093/icb/icq011.

Skyllas, N., M. J. J. E. Loonen, and R. Bintanja. 2023. “Arctic Tern Flyways and the Changing Atlantic Ocean Wind Patterns.” *Climate Change Ecology* 6: 100076. https://doi.org/10.1016/j.ecochg.2023.100076.

Somveille, M., M. P. Dias, H. Weimerskirch, and T. E. Davies. 2020. “Projected Migrations of Southern Indian Ocean Albatrosses as a Response to Climate Change.” *Ecography* 43, no. 11: 1683–1691. https://doi.org/10.1111/ecog.05066.

Suchy, K. D., K. Young, M. Galbraith, R. I. Perry, and M. Costa. 2022. “Match/Mismatch Between Phytoplankton and Crustacean Zooplankton Phenology in the Strait of Georgia, Canada.” *Frontiers in Marine Science* 9: 1–22. https://doi.org/10.3389/fmars.2022.832684.

Vansteelant, W. M. G., J. Shamoun-Baranes, W. van Manen, J. van Diermen, and W. Bouten. 2017. “Seasonal Detours by Soaring Migrants Shaped by Wind Regimes Along the East Atlantic Flyway.” *Journal of Animal Ecology* 86, no. 2: 179–191. https://doi.org/10.1111/1365-2656.12593.

Volkov, A. E., M. J. J. E. Loonen, E. V. Volkova, and D. A. Denisov. 2017. “New Data for Arctic Terns (Sterna Paradisaea) Migration From White Sea (Onega Peninsula).” *Ornithologia* 41: 58–68.

Ward, R. M. 2000. “Migration Patterns and Moult of Common Terns *Sterna Hirundo* and Sandwich Terns *Sterna Sandvicensis* Using Teesmouth in Late Summer.” *Ringing & Migration* 20, no. 1: 19–28. https://doi.org/10.1080/03078698.2000.9674223.

Weber, T. P., B. J. Ens, and A. I. Houston. 1998. “Optimal Avian Migration: A Dynamic Model of Fuel Stores and Site Use.” *Evolutionary Ecology* 12: 377–401. https://doi.org/10.1023/A:1006560420310.

Wernham, C. 2002. *The Migration Atlas: Movements of the Birds of Britain and Ireland*. T. & A.D. Poyser.

Wynn, R. B., D. Brown, G. Thomas, et al. 2014. “Spring Migration Routes of Long-Tailed Skuas Around and Across the UK – Results of Observational and Tracking Data.” *British Birds* 107: 220–228.

Yoda, K., T. Yamamoto, H. Suzuki, S. Matsumoto, M. Müller, and M. Yamamoto. 2017. “Compass Orientation Drives Naïve Pelagic Seabirds To Cross Mountain Ranges.” *Current Biology* 27, no. 21: R1152–R1153. https://doi.org/10.1016/j.cub.2017.09.009.

Supporting Information

Additional supporting information can be found online in the Supporting Information section.